CORRIGENDUM

HALDUN KARAN

Geosystems Research Institute, Mississippi State University, Starkville, Mississippi

PATRICK J. FITZPATRICK AND CHRISTOPHER M. HILL

Northern Gulf Institute, Stennis Space Center, Mississippi

YONGZUO LI

Center for Analysis and Prediction of Storms, University of Oklahoma, Norman, Oklahoma

QINGNONG XIAO AND EUNHA LIM

College of Marine Science, University of South Florida, St. Petersburg, Florida, and National Center for Atmospheric Research, Boulder, Colorado

(Manuscript received 18 October 2010, in final form 30 November 2010)

Incorrect surface observation data are displayed in some of the figures in Karan et al. (2010). Figures 1, 3, 12, and 19 in Karan et al. (2010) incorrectly show data from 5 h after the labeled time. The figures are revised and shown here as Figs. 1–4, respectively, with correct surface observations. Corrections to the original text are shown below.

In the original manuscript, it was indicated that the surface flow just ahead (east) of the cold front was northwesterly, similar to the flow behind the cold front. Instead, the environmental flow ahead of the cold front was southwesterly with stronger, more southerly and southeasterly flow present along the Texas and Louisiana coastlines.

In place of the third and fourth sentences on p. 244, the text should read as follows: ''Apparent northwesterly flow behind, and south-to-southwesterly flow ahead of the CF converge colder, drier air from the north, with warmer, moister air from the Gulf of Mexico.''

A similar statement should replace the last statement on p. 252. The third sentence of the last paragraph on p. 256 should be replaced with, ''The northeast–southwest-oriented line of clouds east of the front appears to move relatively faster than the surface cold front.'' Since surface synoptic-scale observations did not indicate any pressure variations associated with this upper-level disturbance, and since the Houston–Galveston, Texas (KHGX), velocity–azimuth display (VAD) analysis indicates such a flow disturbance at 1.5–1.8 km AGL, we prefer to refer to this disturbance ahead of the cold front not as a low-level trough passage, as mentioned in several places in the original manuscript, but rather as an upper-level disturbance. The second sentence on p. 257 should read: ''Temporal resolution of surface observations is not adequate for resolving this fast-moving upper-level disturbance.''

REFERENCE

Karan, H., P. J. Fitzpatrick, C. M. Hill, Y. Li, Q. Xiao, and E. Lim, 2010: The formation of multiple squall lines and the impacts of WSR-88D radial winds in a WRF simulation. *Wea. Forecasting,* **25,** 242–261.

Corresponding author address: Haldun Karan, Geosystems Research Institute, Rm. 219, 2 Research Blvd., Starkville, MS 39759. E-mail: karan@gri.msstate.edu

DOI: 10.1175/WAF-D-10-05035.1

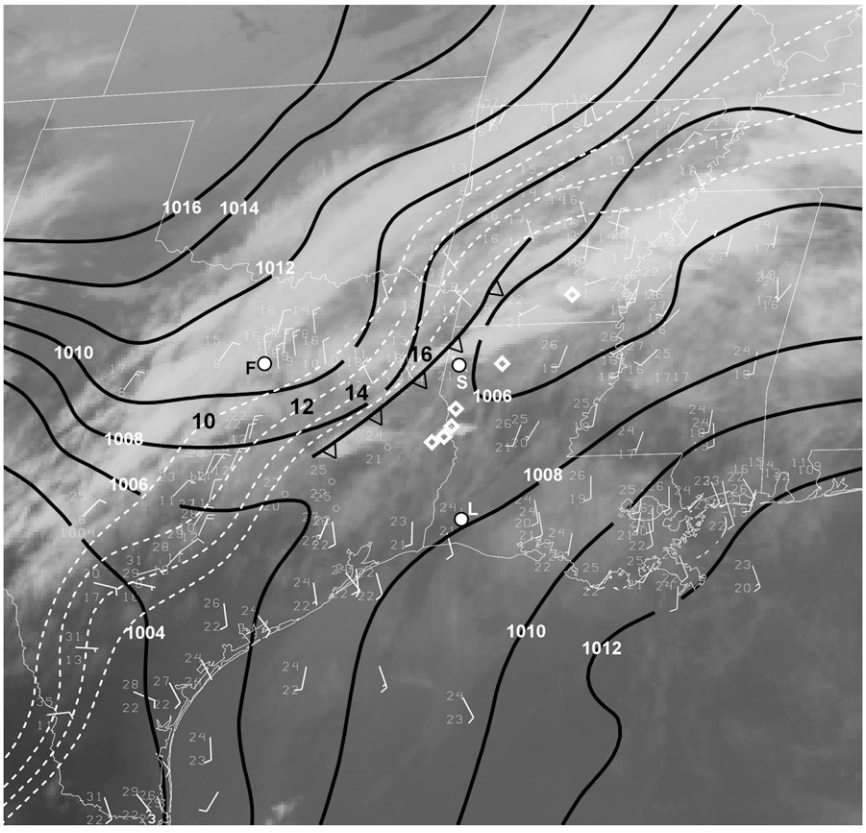

FIG. 1. Corrected version of Fig. 1 in Karan et al. (2010). Surface observations at 0000 UTC 30 Apr overlaid on a *Geostationary Operational Environmental Satellite-12* (*GOES-12*) IR image at 2345 UTC 29 Apr 2005. The Dallas–Fort Worth, TX (KFWS, F); Shreveport, LA (KSHV, S); and Lake Charles, LA (KLCH, L) radars are depicted with circles and letters. The KSHV radar *Z* field is used for locations of the intense convective cells (depicted with diamonds) within the developing squall line. KSHV-observed radar finelines are used to locate the cold front (CF) position. The white dashed lines represent the dewpoint temperature contours, varying between 10° and 12°C within and behind the CF. The isobars are depicted with solid lines. Full and half barbs represent 10- and 5-kt winds (2.5 and 5 m s^{-1}), respectively.

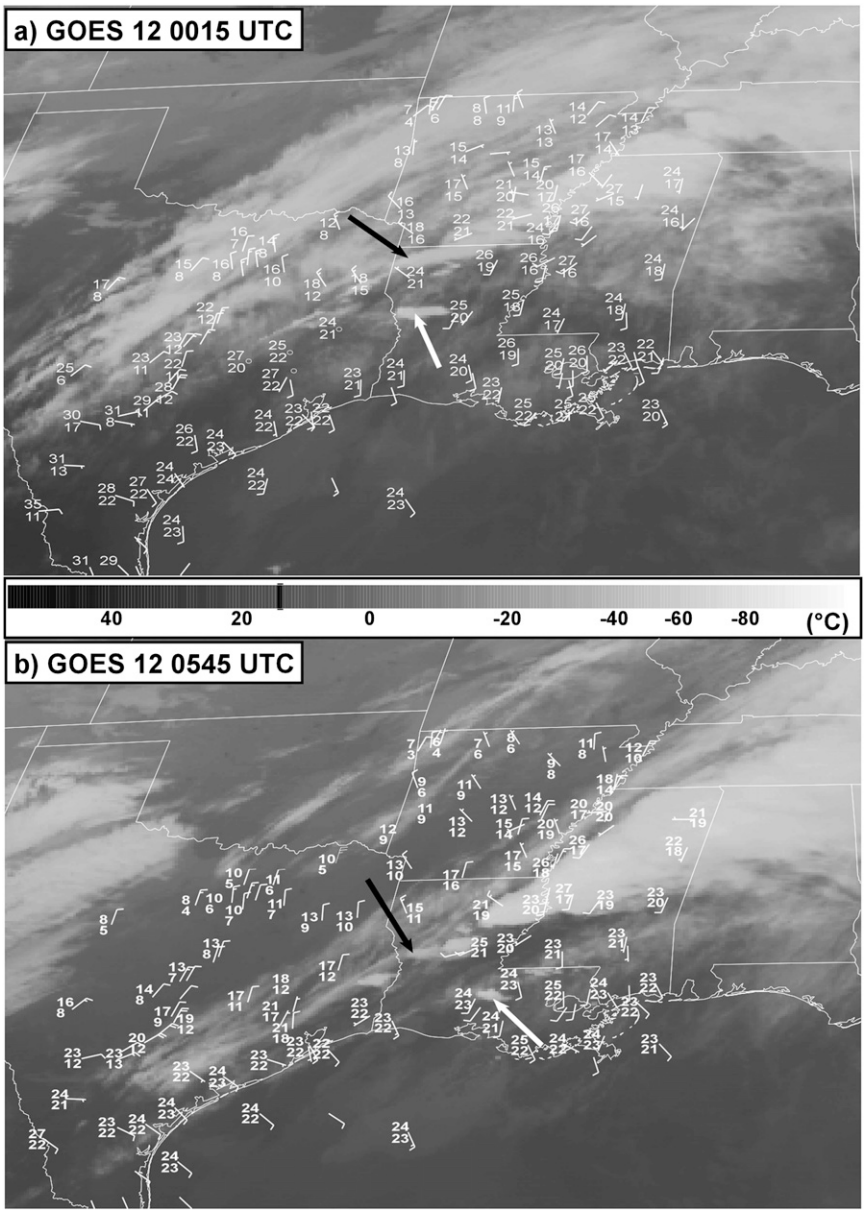

FIG. 2. Corrected version of Fig. 3 in Karan et al. (2010). *GOES-12* IR derived brightness temperatures at (a) 0015 and (b) 0545 UTC. The black arrows and the white arrow in (a) depict the line of convection associated with the CF and the initial formation of the primary squall line, respectively. The white arrow in (b) indicates deep cloud development associated with the secondary squall line.

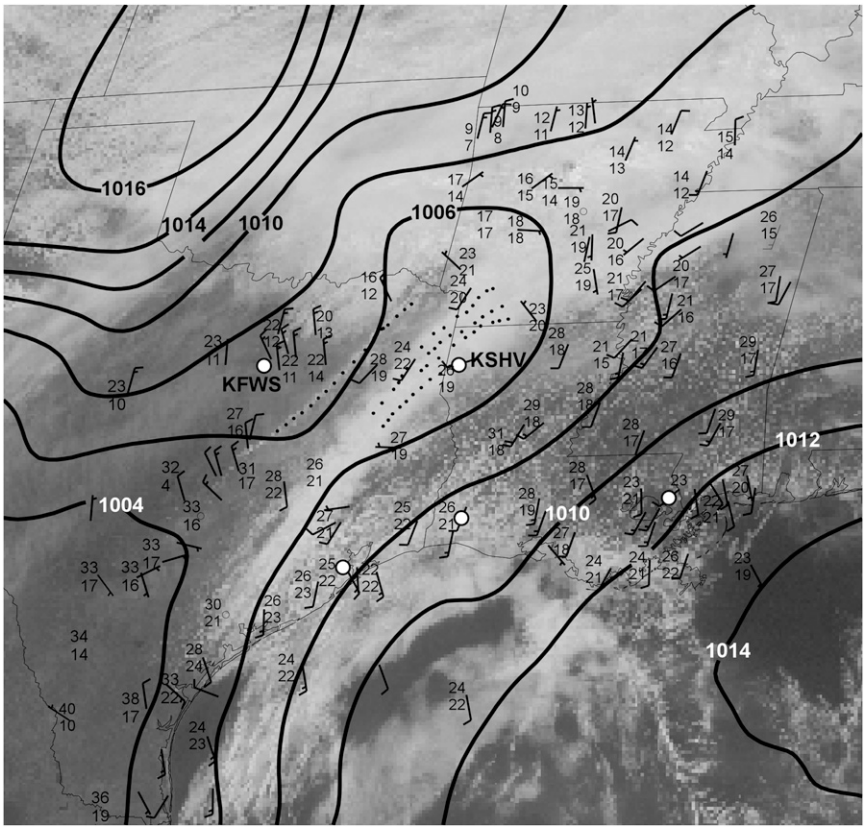

FIG. 3. Corrected version of Fig. 12 in Karan et al. (2010). Surface observations at 2000 UTC overlaid on a *GOES-12* visible image at 1945 UTC 29 Apr 2005. Solid contours show the isobars. Full barbs represent 10-kt winds. White circles depict the Weather Surveillance Radar-1988 Doppler (WSR-88) stations at KFWS and Galveston in TX, and at Lake Charles, Slidell, and KSHV in LA. The westernmost dotted line is the CF location. The dotted lines east of the CF depict the gravity waves.

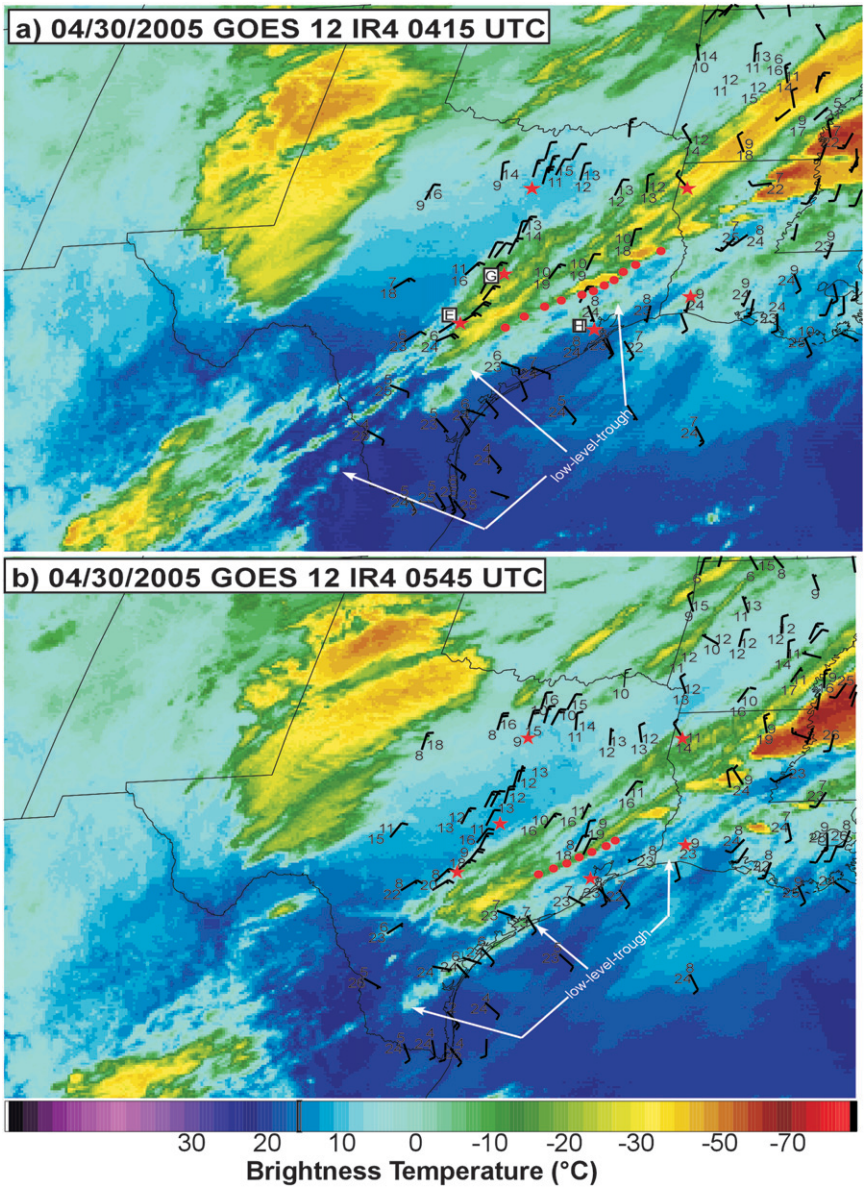

FIG. 4. Corrected version of Fig. 19 in Karan et al. (2010). (a) Brightness temperatures at 0415 UTC 30 Apr 2005 with surface and buoy observations valid at 0500 UTC. The red dots depict the location of the CF observed as a radar fineline delineated by the KHGX radar at 0411 UTC from the lowest elevation angle. The (pressure − 1000 hPa) and temperature values are depicted in the upper-right and lower-left corners at each stations, respectively. Full barbs represent 10-kt winds. (b) As in (a), but for the 0545 UTC *GOES-12* IR image and 0600 UTC surface and buoy observations. The KHGX data at 0544 UTC from the lowest elevation angle were used to locate the fineline associated with the CF. The letters E, G, and H (with stars) depict the locations of the Austin–San Antonio, TX (KEWX); Fort Hood, TX (KGRK); and KHGX Doppler radars. White arrows point to an upper-level disturbance.